Egyptian Journal of Chemistry
http://ejchem.journals.ekb.eg/

Molecular Electrostatic Potential Mapping for PANI Emeraldine Salts and Ag@PANI core-shell

Neveen M. Farrage[1], Ahmed H. Oraby[2], Elmetwally M. Abdelrazek[2] and Diaa Atta[1*]

[1]*Spectroscopy Department, National Research Centre, 33 El-Bohouth St., 12622, Dokki, Giza, Egypt.*

[2]*Physics Department, Faculty of Science, Mansoura University, Mansoura, 35516, Egypt.*

THE quantum mechanical calculations have been utilized using the density function theory (DFT) byB3LYP method on the basis set 6-31g(d,p) to calculate the single point energy of Polyaniline emeraldine nitrate salt (PANI-nitrate). Polyaniline emeraldine sulphate (PANI-Sulphate) was also calculated on the same level. At the end the Ag@PANI-nitrate core-shell was calculated on the same level of calculations. For the previously named structures,the total dipole moment vector of every molecule was also calculated in addition to the energy band gap between the highest occupied molecular orbital (HOMO) and the lowest occupied molecular orbital (LUMO) and the distribution of the Electrostatic potential. More investigations for the studied molecules have been done in the presence of water molecules.

Keywords: Single point energy, DFT, Ag@PANI core-shell, HOMO-LUMO, Electrostatic potential mapping, Total electron density.

Introduction

Polymers are one from the main and important materials, that are divided in families like the semi flexible rod family[1,2]. One from the most important polymers is the Polyaniline (PANI) which is a member in the semi flexible rod family [3,4] and is a product of the polymerization of the aniline monomer. While it was discovered from more than a century ago exactly in 1862 by Leitch,it is being intensively investigated from the time of discovery of its electrical properties and its good electrical conductivity. Because of its high electrical conductivity, and the simplicity of its production, PANI and PANI derivatives have been used in the intelligent products like intelligent multifunction yarn and super capacitors [5,6]. PANI is also unique in its stability which is in the polymer's world is a limiting factor. Preparation of the PANI could be done by different methods, in total all could be regarded as one from the simplest polymers in syntheses, however as its synthesis is simple, its chemical reactions are complex.

After long time from its discovery PANI, got great attention from the scientists. The one could easily observe that PANI is the most conducting polymer investigated over the last two decades. PANI has different forms from the point of view of its oxidation states like Leuco-emeraldine, Emeraldine and Pernigraniline. The molecular conformation effect on the oxidation reduction state has confirmed that Leuco-emeraldine is fully reduced, Pernigraniline is fully oxidized and emeraldine is neutral. Meaning that emeraldine is partially in oxidation and partially in reduction state [7,8]. The most stable and conducting PANI conformer under room temperature is the emeraldine base, while the other conformers could be regarded as insulators. Molecular modeling is a new approach that emerged in the last two decades of the last century and rapidly became one from the most important tools in the scientific research in many branches like chemistry, physics, pollution and environment, pharmacology, etc. [9-11]. The definition of the Molecular modeling

*Corresponding author e-mail: Diaalolo2004@yahoo.com
Received 28/2/2019; Accepted 17/5/2019
DOI: 10.21608/ejchem.2019.12746.1791
©2019 National Information and Documentation Center (NIDOC)

is the application of the chemistry and quantum mechanics laws using [12] strong computing systems with such support from experimental data as confirmation of the correctness of the given molecularstructure model. The advancement in Molecular modeling depends strongly on the advancement in the theoretical aspects and the calculation facilities. By molecular modeling one could explain several chemical, Physical and biological processes related to the 3D structure of the molecule. In that sense molecular modeling or molecular simulation became an important tool for studying the physical, biological and chemical behavior of the under investigation molecular system [13-18]. By means of molecular modeling one can calculate several parameters like the bond angle, bond length, the vibrational spectra [19], electronic transitions and the electrostatic potential [20,21] around the studied molecule. Emeraldine salts are one from the most investigated PANI compounds.

One can conclude that the meaning of what is called the single point energy is the overall sum of energy of such fixed nucleus molecule. If the nucleus is clamped in the space to a specific location, hence it is called nucleus clamping approximation [22,23]. The quantum mechanical approximation done by Born and Oppenheimeris resembling only single point from the potential energy (P.E) outer distribution that yields what is called the single point energy [24]. Simply this approximation separates the motion of both the nucleus and the electrons. By means of mathematics, one can write the single point energy or the P.E. surface as the total addition of all electronic energy (E_e) plus the nuclear repulsion P.E(V_{nn}) as follows [25,26]

$$V(R) = E_e + V_{nn}$$

one can get the electronic energy by solving the electronic section of Schrödinger equation [26]

$$\hat{H}_e \psi_e(r;R) = E_e \psi_e(r;R)$$

Molecular electrostatic potential (MEP) mapping is a useful tool to predict the chemical reactivity of such molecule.In this kind of calculation, a grid cube is utilized to calculate total electron density around the investigated molecule.The MEP surface could be defined as the region that no other molecule could penetrate or in other words it is the nearest distance that no other molecule could approach [27].

What we desire is not only to map the electron density around the studied molecules, but to determine the MEP surface. The characterization techniques of the polymers and nanostructures in scientific research work are depending mainly on the molecular spectroscopic tools like FTIR and Raman [28,29], together with the imaging techniques like electron microscopy and optical microscopic tools [30,31]. Molecular modeling has its importance that leads to understanding the recorded spectra and the detected images. In a previous work preparation by solid state reaction and experimental characterizations for PANI salts and P Ag@PANI core-shell have been presented. In this work, the single point energy was calculated for PANI emeraldine, PANI sulphate, PANI nitrate and PANI silver nitrate core-shell. The studied structures have been calculated in gas phase and in presence of water molecules. The quantum mechanical DFT is utilized in this calculation as the most precise level of calculations. Some physical and electronical parameters that has been excreted from the calculated model, are illustrated in this paper.

Calculation Details

All calculations were done by using Gaussian 03 [32], we used a PC to carry out the molecular modeling calculations at National Research Centre, physics division, spectroscopy department.

The optimization of the PANI molecule have been done (DFT) using B3LYP method and 6-31g(d,p) basis set. The Single point energy calculations were done and the structure has been studied with DFT using B3LYP method and 6-31g (d,p)basis set [33-35].

At the same calculation of the total dipole moment, the highest occupied molecular orbital and the lowest occupied molecular orbital (HOMO/LUMO)have been calculated. Moreover, the bandgap energy or in other words the difference between the HOMO and LUMO (ΔE_g) is also calculated by the DFT theory with the same method and basis set.

By means of Gaussian, the molecular electrostatic potential has been calculated for the studied molecules, and the maximum MEP determined for each. In the presented MEP mapping the blue color refers to the extremely positive charge and the red one is indicator for the extreme negative charge.

Results and Discussion

The optimized structure of PANI emeraldine and the calculated frequency are shown in Fig. 1-a and 1-b respectively. Fig. 1-c and 1-d show a comparison between the MEP mapping for the optimized structure and that for the single point energy calculations. It is clear that in our case the optimization did not affect the electrostatic potential distribution, moreover the maximum MEP approximately the same for both methods, that for the optimized structure it was found to be 30.416 $\times 10^{-2}$(*au*) while for the single point energy calculation it was found to be 30.499 $\times 10^{-2}$(*au*).

The Single point energy of the PANI emeraldine in gas phase and in the presence of water molecules shown in section (a) of Fig 2,3 and 4 have been calculated by DFT using B3LYP method and 6-31g (d,p) basis set. For the same structures the HOMO-LUMO distribution was calculated and shown in section (b) of Fig. from 2 to 4 respectively. The molecular electrostatic potential distribution around the studied structures for the PANI in the 3 studied cases is illustrated in section (c) from Fig. 2,3 and 4. Section (d) in the previous Fig. present the total dipole moment vector for the molecules at the same level of calculations. As it is clear from table 1 the total dipole moment changed by the increase of the amount of water molecules around the PANI molecule, while it was less than one Debye in the gas phase it increased to 4.8513 Debye in the case of two water molecules. The presence of four water molecules doubled the total dipole moment, but it did not affect the band gap energy of the PANI molecule. On the other hand, the band gap energy was not affected by the presence of water molecules as listed in table 2.

The maximum value of MEP has increased by the increase of the water molecule around the PANI molecule but without much effect, it changed from 11.1060$\times 10^{-2}$*au* up to 11.8664 $\times 10^{-2}$*au*. PANI sulphate single point energy have been calculated also by DFT theory on the same level of calculation in the presence of five water molecules as shown in Fig.5. In section (a) the structure geometry is presented while the HOMO-LUMO distribution comes in section (b). The Electrostatic potential distribution illustrated in section (c) from the same Fig., the total dipole moment is shown in Fig.5(c).

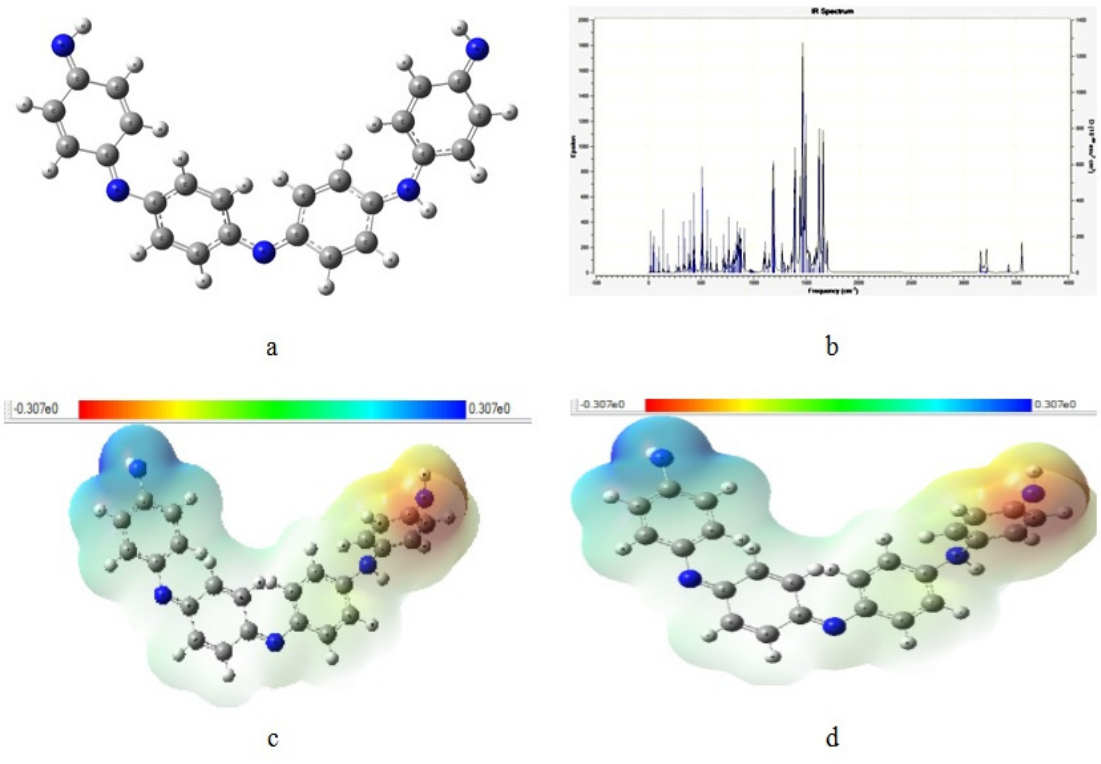

Fig. 1. a) The optimized structure, b) IR, c) Electrostatic potential distribution for the optimized structure, d) Electrostatic potential distribution for the single point energy calculations of PANI in gas phase calculated by DFT using B3LYP method at 6-31g (d,p)basis set.

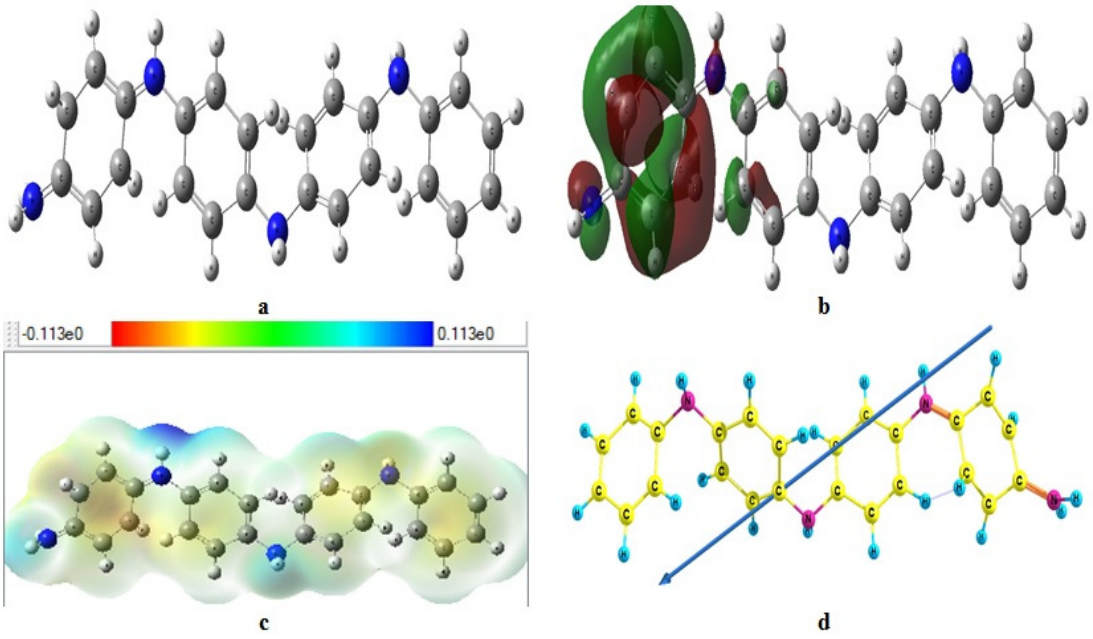

Fig. 2. a) Single point energy, b) HOMO-LUMO distribution, c) Electrostatic potential distribution, d) The total dipole moment vector of PANI in gas phase calculated by DFT using B3LYP method at 6-31g (d,p) basis set.

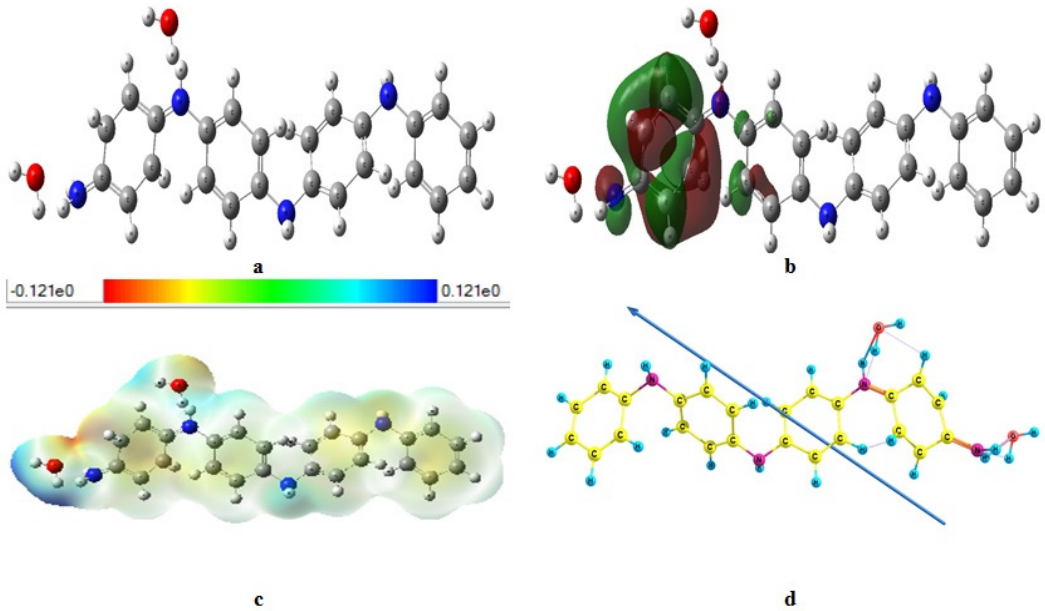

Fig. 3. a) Single point energy, b) HOMO-LUMO distribution, c) Electrostatic potential distribution, d) The total dipole moment vector of PANI in the presence of two water molecules calculated by DFT using B3LYP method at 6-31g (d,p) basis set.

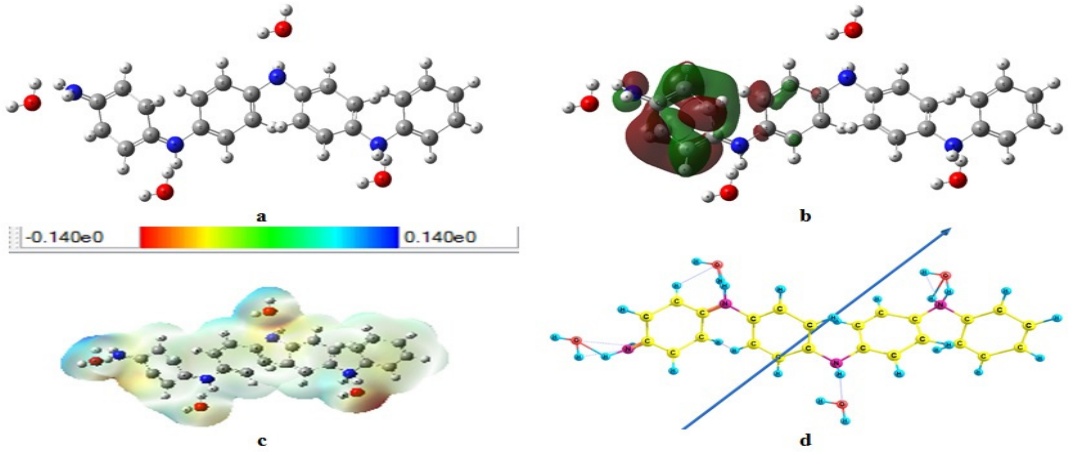

Fig. 4. a) Single point energy, b) HOMO-LUMO distribution, c) Electrostatic potential distribution, d) The total dipole moment vector of PANI in the presence of four water molecules calculated by DFT using B3LYP method at 6-31g (d,p) basis set.

TABLE 1. The calculated total dipole moment vector of the studied molecules by DFT on B3LYP method and 6-31g (d,p) basis set.

Compound	Total Dipole moment			Magnitude (Debye)
	X-component	Y- component	Z- component	
PANI Gas state	-0.7908	0.4299	-0.0857	0.9042
PANI two water molecule	-4.0826	-2.6193	0.0841	4.8513
PANI four water molecule	-7.0953	6.9895	-0.4503	9.9699
PANI mono sulphate with 5 water molecules	5.3016	8.5065	-1.3321	10.1115
PANI di sulphate with 6 water molecules	-0.4756	5.2794	-4.0492	6.6704
PANI mono nitrate with 5 water molecules	-9.0873	1.5480	-1.8115	9.3945
PANI di nitrate with 6 water molecules	11.2916	1.8164	0.5488	11.4499
Ag@PANI-nitrate core-shell with 18 water molecules	90.3151	0.5490	-22.5993	93.1013

TABLE 2 The calculated band gap energy and MEP maximum of the studied molecules by DFT using B3LYP method at 6-31g (d,p) basis set.

Compound	Band gap Energy(*ev*)	Maximum MEP×10^{-2}(*a*u)
PANI Gas state	2.48850082	11.1060
PANI two water molecule	2.48033734	11.6769
PANI four water molecule	2.479520992	11.8664
PANI mono sulphate with 5 water molecules	2.021005532	16.8306
PANI di sulphate with 6 water molecules	0.413888436	14.0723
PANI mono nitrate with 5 water molecules	0.758659408	26.8513
PANI di nitrate with 6 water molecules	0.910772252	22.7388
Ag@PANI-nitrate core-shell with 18 water molecules	1.392961804	15.77

* According to the calculations the selected is o value is 0.0004

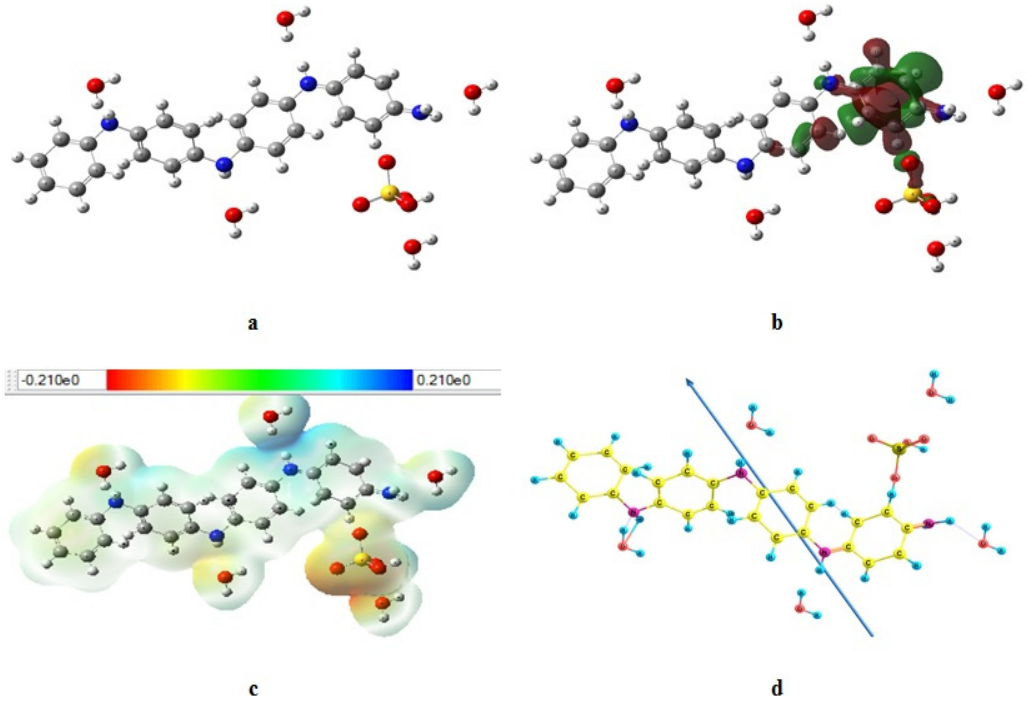

Fig. 5. a) Single point energy, b) HOMO-LUMO distribution, c) Electrostatic potential distribution, d) The total dipole moment vector of PANI mono sulphate in the presence of five water molecules calculated by DFT using B3LYP method at 6-31g (d,p) basis set.

The total dipole moment of the PANI mono sulphate is 10.1115 Debye while the band gap energy decreased slightly from 2.48850082 *ev* in the case of PANI in gas phase to 2.02100553 *ev*. The presence of sulphate group increases the max MEP from around 11.8×10^{-2}*au* up to 16.8306×10^{-2}*au*.

Fig. 5 presents the PANI di-sulphate surrounded by 6 water molecules, like the previous structures the single point energy, HOMO-LUMO, Electrostatic potential and the total dipole moment are shown in sections a, b, c and d respectively. In this case the duplication of sulphate molecules increases the conductivity of the poly aniline molecule by decreasing the band gap energy to 0.41388436 *ev*. Also, in this regime the max MEP decreased to 14.0723×10^{-2} *au* as presented in table 2, while the total dipole moment has increased from around 0.9 Debye in the case of PANI in gas phase to 6.6704 Debye. As stated before, the decrease in the band gap energy and increase in total dipole moment is a strong indication about the enhancement of the compound reactivity.

The same effect takes place in the case of the nitrate compounds which are presented in Fig.7 and 8. The enhancement in case of PANI nitrate is clearly more than that in the PANI sulphate and is clear from the total dipole moment which becomes 11.4499 Debye for the PANI sulphate. Like in sulphate there are tremendous decrease in the band gap energy reaching to 0.758659408 *ev* in the case of mono-nitrate PANI and increasing slightly to 0.910772252 *ev* for the di-nitrate PANI. Like what happened in sulphate, the increase of the nitrate groups affects the Max. MEP which decreases from 26.8513×10^{-2}*au* in the presence of single nitrate group to 22.7388×10^{-2}*au*. when the nitrate group get doubled.

Finally, the model molecule of Ag@PANI-nitrate core-shell is shown in Fig.9. The core-shell structure is considered as nano structure its reactivity increased significantly while the total dipole moment jumped up to 93.1013 Debye. The calculated band gap energy of the core-shell is 1.392961804 as the max. calculated MEP is 15.77×10^{-2}*au*.

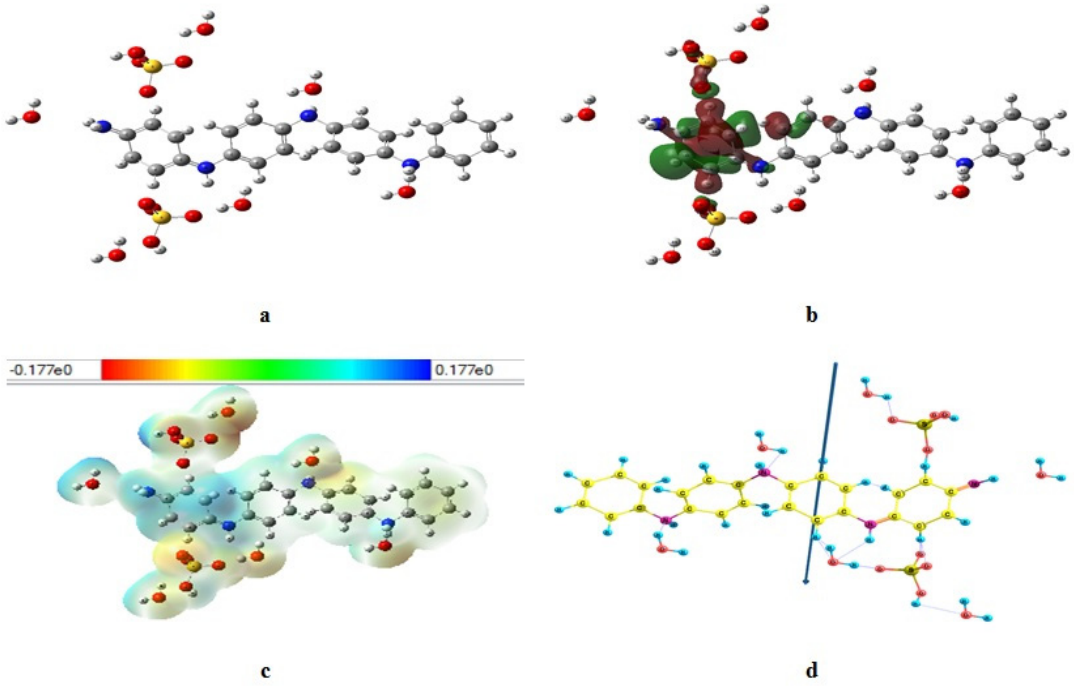

Fig. 6. a) Single point energy, b) HOMO-LUMO distribution, c) Electrostatic potential distribution, d) The total dipole moment vector of PANI di sulphate in the presence of six water molecules calculated by DFT using B3LYP method at 6-31g (d,p) basis set.

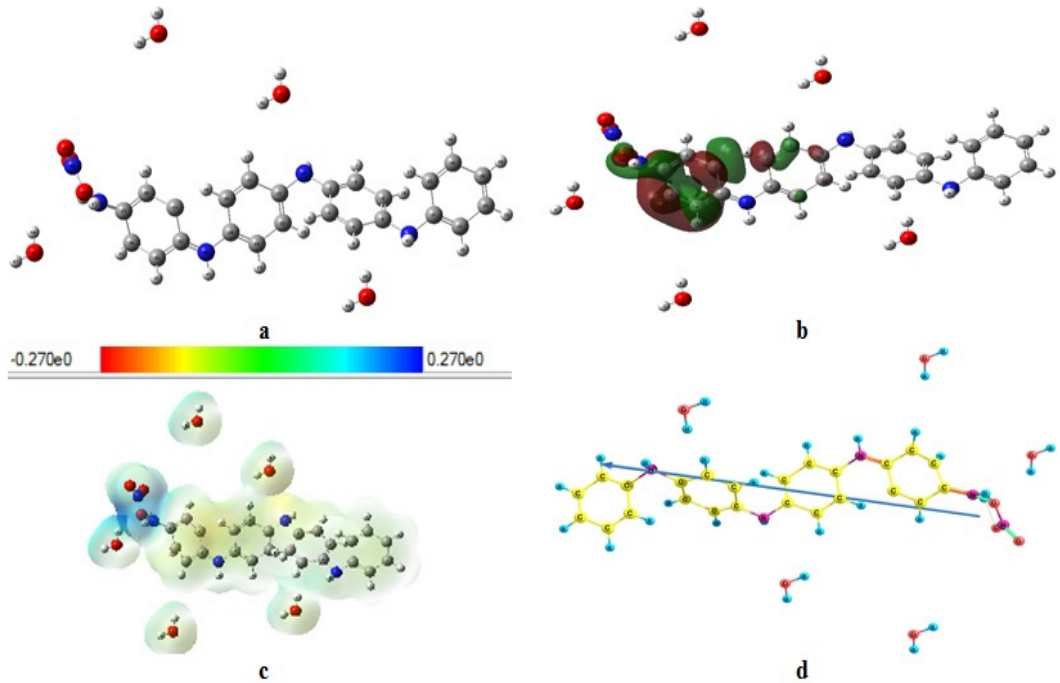

Fig. 7. a) Single point energy, b) HOMO-LUMO distribution, c) Electrostatic potential distribution, d) The total dipole moment vector of PANI mono nitrate in the presence of five water molecules calculated by DFT using B3LYP method at 6-31g (d,p) basis set.

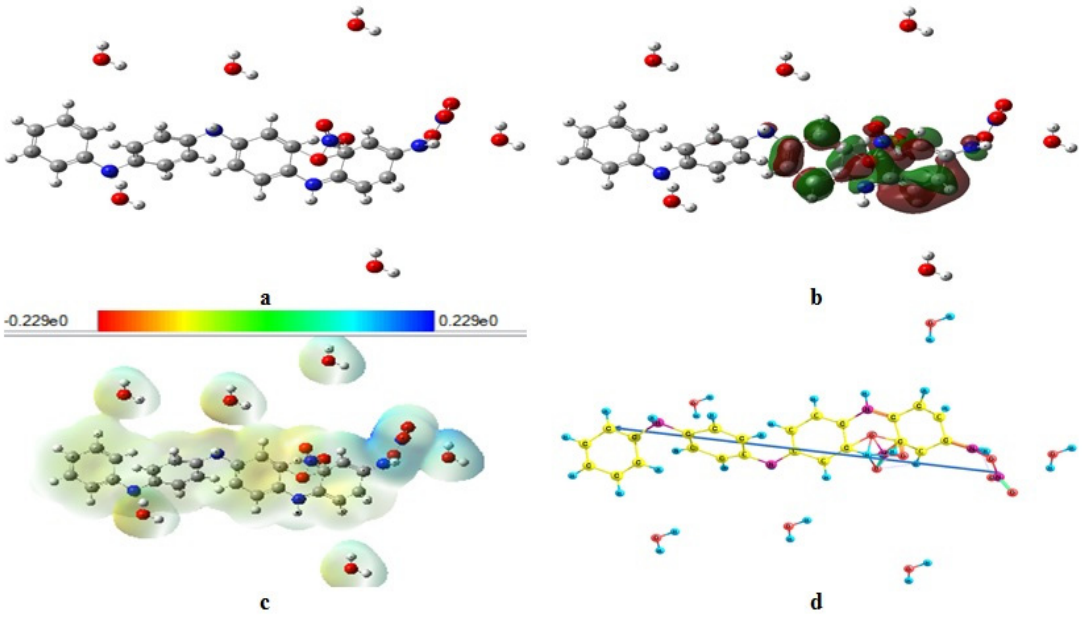

Fig. 8. a) Single point energy, b) HOMO-LUMO distribution, c) Electrostatic potential distribution, d) The total dipole moment vector of PANI di nitrate in the presence of six water molecules calculated by DFT using B3LYP method at 6-31g (d,p) basis set.

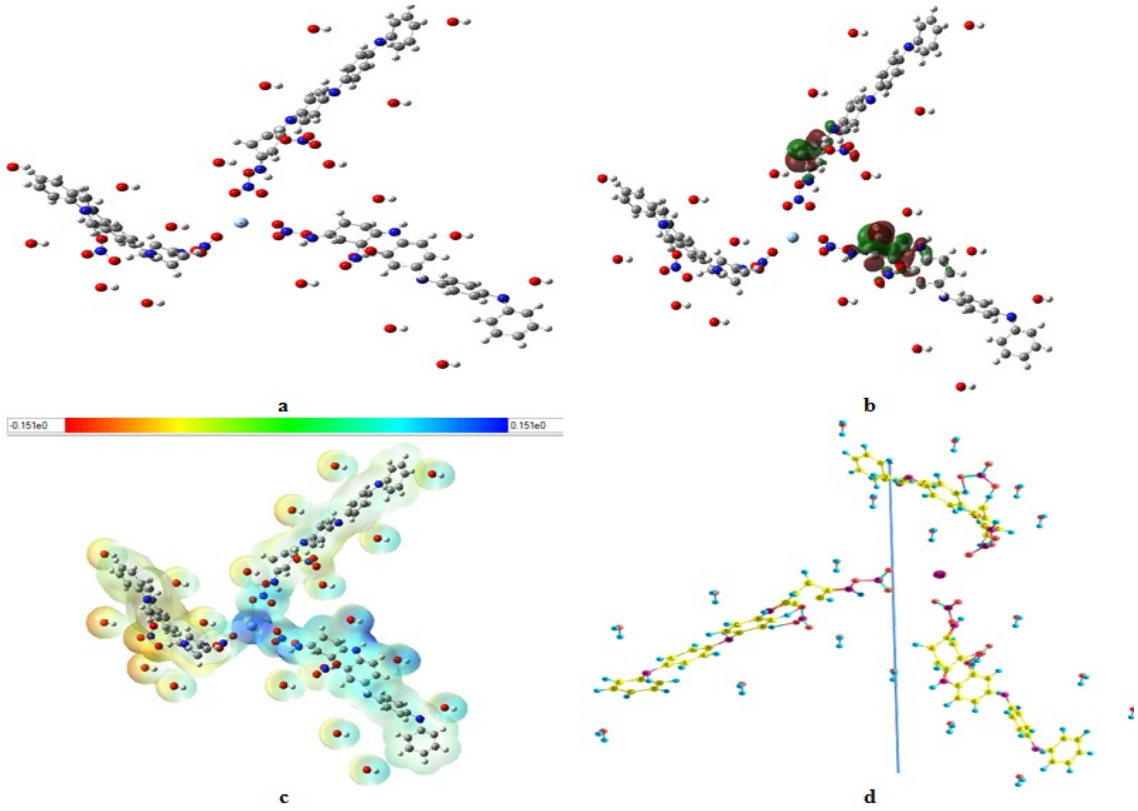

Fig. 9. a) Single point energy, b) HOMO-LUMO distribution, c) Electrostatic potential distribution, d) The total dipole moment vector of PANI-nitrate@Ag core-shell in the presence of eighteen water molecules calculated by DFT using B3LYP method at 6-31g (d,p) basis set.

Conclusion

The structure studies of the PANI confirm that the emeraldine salts has higher conductivity and higher reactivity. While the shell structure of PANI-nitrate around a silver core have a formidable increase in the reactivity, this also was clear from the distribution of the electrostatic potential surface of the studied molecules. The discussed results prove that the Ag@PANI core-shell is recommended to be used in applications which need high conductor polymer, also as a good sensor for the bioactivity.

Acknowledgement

The authors would like to deeply acknowledge Prof. Medhat A. A. Ibrahim, Professor of Applied Spectroscopy in Spectroscopy Department, National Research Centre, Cairo, Egypt for his kind help in the calculations and introducing his lab facilities. we also want to thank Prof. Dr. Ahmed Fakhry for his support in manuscript revision and his fruitful advices.

References

1. Sergei A.E., Hsiao-Ping H., Andrey M. and Kurt B., Semiflexible polymer brushes and the brush-mushroom crossover, *Soft Matter*, **11**, 2604-2616 (2015).
2. Chetna D., Maumita D., Monika D. and Malhotra B.D., Recent advances in polyaniline based biosensors, *Biosen Bioelectron*, **26**, 2811-2821 (2011).
3. MohsenR.M., MorsiS.M.M., Abu-AyanaY.M. andGhoneim A.M., Synthesis of Conductive Cu-core/Ag-subshell/polyaniline-shell Nanocomposites and their Antimicrobial Activity, *Egypt. J. Chem.*, **61**, 939-952 (2018).
4. Ramadan M.A., FathiA., Shaarawy S. and El-bisi M., A New Approach for Preparation of Smart Conductive Textiles by Polyaniline through in-situ Polymerization Technique, *Egypt. J. Chem.*, **61**, 479-492 (2018).
5. Shaohua W., Penghong L., Yue Z., Hongnan Z. andXiaohong Q., Flexible and conductive nanofiber-structured single yarn sensor for smart wearable devices, *Sensor Actuat. B-Chem.*, **252**, 697-705 (2017).
6. Wang K., Meng Q., Zhang Y., Wei Z. and Miao M., High performance two-ply yarn supercapacitors based on carbon nanotubes and polyaniline nanowire arrays, *Adv. Mater.*, **25**, 1494-1498 (2013).
7. Wang Z., Wang H., Wu J., Zhou C. and Xin B., Promoted effect of pernigraniline as electrons accepter on RhB degradation over TiO2/ITO film, *J.Nanosci.Nanotechno.*, **17**, 2666-2673 (2017).
8. Xiaoyan M., Guangying Z. andWenchao D., Electropolymerization of stable leucoemeraldine base polyaniline film and application for quantitative detection ofEscherichia coliO157:H7, *J. Electron. Mater.*,**47**, 6507–6517 (2018).
9. Ibrahim M., Elhaes H. and Atta D., Computational notes on the effect of sodium substitution on the physical properties of fullerene, *J. Comput. Theor. Nanosci.,* **14**, 4114-4117 (2017).
10. Atta D., Gomaa F., Elhaes H. and Ibrahim M., Effect of hydrated dioxin on the physical and geometrical parameters of some amino acids, *J.Comput.Theor. Nanosci.*, **14**, 2405-2408 (2017).
11. Okasha A., Atta D., Badawy W.M., FrontasyevaM.V., Elhaes H. and Ibrahim M., Modeling the coordination between Na, Mg, Ca, Fe, Ni, and Zn with organic acids, *J. Comput. Theor. Nanosci.,* **14**, 1357-1361 (2017).
12. Foresman J.B. and Frisch A., Exploring chemistry with electronic structure methods. 2nd Ed., Gaussian Inc., Pittsburgh, PA (1996)
13. Jiao G., Xin Y., Yajing Z., Yinhe S. and Xin P., Binding studies of triclocarban with bovine serum albumin: Insights from multi-spectroscopy and molecular modeling methods, *Spectrochim. Acta A*, **202**,1-12 (2018).
14. Rabelo V.W., Santos T.F., Terra L., Santana M.V., Castro H.C., Rodrigues C.R., Abreu P.A., Targeting CYP51 for drug design by the contributions of molecular modeling. *Fundam. Clin. Pharmacol.*, **31**, 37-53, (2017).
15. Tripti D., Ravi S., Ramesh P., Ankit H., Prakram S.C., Subhash J., Anju K., Dharamshibhai R. and Chaitanya J., Cloning, molecular modeling and characterization of acidic cellulase from buffalo rumen and its applicability in saccharification of lignocellulosic biomass, *Int. J. Biol.Macromol.*, **113**, 73-81 (2018).
16. Atta D., Gomaa F., Elhaes H. and Ibrahim M., On the molecular modeling analyses for the effect of hydrated dioxin upon organic acids, *Energy Environ. Focus*, **5**, 295–298 (2017).
17. Saugat A., Saloni D., Filip F., Miguel R., Suman S., Kenneth A. and Sai H.S.B., Elucidation of the orientation of selected drugs with 2-hydroxylpropyl-β-cyclodextrin using 2D-NMR spectroscopy and molecular modeling, *Int. J.Pharmaceut.*, **545**, 357-365 (2018).

18. Krüger A., Zimbres F. M., Kronenberger T. andWrenger C., Molecular modeling applied to nucleic acid-based molecule development,*Biomolecules*, **8**, 83 (2018).

19. Atta D., Refaat A., Fahmy A., Ibrahim M., Elhaes H. and Ibrahim M., Spectroscopic analysis of cross linked sodium alginate composites, *Materials Focus*, **6**, 618-624 (2017).

20. Samiran P., Tanusri D. and Alok K.M., Five benzoic acid derivatives: Crystallographic study using X-ray powder diffraction, electronic structure and molecular electrostatic potential calculation, *J. Mole. Struct.*, **1175**, 185-194 (2019).

21. Shweta, Eram K., Poonam T., Rakesh M., Padam K., A theoretical study on molecular structure, chemical reactivity and molecular docking studies on dalbergin and methyldalbergin, *J. Mole. Struct.*, **1183**, 100-106 (2019).

22. Rana M.A.K., Fayyaz H., Muhammad I., Rana A.M. and Murtaza G., ab initio study of the exo-hydrogenated single wall carbon nanotubes,*Physica B*,**552**, 124-129 (2019).

23. Yawei C., Xiaoqing Y., Zidong Z. and Wei L., Utilization of generalized energy-based fragmentation method on the study of hydrogen abstraction reactions of large methyl esters, *Combust Flame*, **190**, 467-476 (2018).

24. Grimme S. and Schreiner P.R., Computational chemistry: the fate of current methods and future challenges,*Angew. Chem. Int. Edit.*, **57**, 4170-4176 (2018).

25. Gribov L.A., NovosadovB.K. andProkof'eva N.I., Statement of quantum problems for "hot" molecules and solution of the Schrödinger equation for electron states in the field of distributed nuclear charges, *High.Energ. Chem.*, **47**, 115-119 (2013).

26. Jean D., James E.B. and Attila G.C., Equilibrium molecular structures:from spectroscopy to quantum chemistry, CRC Press, Taylor & Francis, Boca Raton, Florida, USA (2016).

27. Badry R., Shaban H., Elhaes H., Refaat A. and Ibrahim M., Molecular Modeling Analyses of Polyaniline Substituted with Alkali and Alkaline Earth Elements, *Biointerface Research in Applied Chemistry*, **8**, 3719-3724 (2018).

28. Zhihong L., Lihua Z., Yanfei H. andHeqing T., Effects of graphene reduction degree on capacitive performances of graphene/PANI composites, *Synthetic Met.*, **175**, 88-96 (2013).

29. Marcelo M.N., Matteo Ceppatelli C., Marcia L.A.T. and Roberto B., Pressure-induced reactivity in the emeraldine salt and base forms of polyaniline probed by FTIR and Raman, *J. Phys. Chem. C*, **118**, 27559–27566 (2014).

30. Atta D., Okasha A. and Ibrahim M., Setting up and calibration of simultaneous dual color wide field microscope for single molecule imaging, *Der Pharma Chemica*, **8**, 76-82 (2016).

31. Atta D. and Okasha A., Single molecule laser spectroscopy, *Spectrochim. Acta A*, **135**, 1173-1179 (2015).

32. Gaussian 03, Revision B.05,. Frisch M. J, Trucks G. W., Schlegel H. B., Scuseria G. E., Robb M. A., Cheeseman J. R., Montgomery J. A., Vreven Jr. T., Kudin K. N., Burant J. C., Millam J. M., Iyengar S. S., J. Tomasi, V. Barone, B. Mennucci, M. Cossi, G. Scalmani, Rega N., Petersson G. A., Nakatsuji H., Hada M., Ehara M., Toyota K., Fukuda R., Hasegawa J., Ishida M., Nakajima T., Honda Y., Kitao O., Nakai H., Klene M., Li X., Knox J. E., Hratchian H.P., Cross J. B., Adamo C., Jaramillo J., Gomperts R., Stratmann R. E., Yazyev O., Austin A. J., Cammi R., Pomelli C., Ochterski J. W., Ayala P.Y., Morokuma K., Voth G. A., Salvador P., Dannenberg J. J., Zakrzewski V. G., Dapprich S., Daniels A. D., Strain M. C., Farkas O., Malick D. K., Rabuck A. D., Raghavachari K., Foresman J. B., Ortiz J. V., Cui Q., Baboul A. G., Clifford S., Cioslowski J., Stefanov, Liu G., Liashenko A., Piskorz P., Komaromi I., Martin R. L., Fox D. J., Keith T., Al-Laham M. A., Peng C. Y., Nanayakkara A., Challacombe M., Gill P. M. W., Johnson B., Chen W., Wong M. W., Gonzalez C., Pople J. A., Gaussian, Inc., Pittsburgh PA (2003).

33. Vosko S.H.,Wilk L. andNusair M., Accurate spin-dependent electron liquid correlation energies for local spin density calculations: a critical analysis, *Can. J. Phys.*, **58**, 1200-1211 (1980).

34. Becke A., Density-functional exchange-energy approximation with correct asymptotic behavior, *Phys. Rev. A*, **38**, 3098-30100 (1988).

35. Lee C., Yang W. and Parr R.G., Development of the Colle-Salvetti correlation-energy formula into a functional of the electron density, *Phys. Rev. B*, **37**, 785-789 (1988).

توزيع الجهد الكهربى الساكن حول جزيئات املاح البولى انيلين ايمرالدين و جزىء الفضة بولى انيلين كور-شيل

نيفين محمد فراج[1], احمد حمزة عرابى[2], المتولى عبد الرازق[2], ضياء الدين عطا[1]

[1] قسم الطيف- شعبة البحوث الفيزيقية- المركز القومى للبحوث- الدقى-القاهرة -12622 مصر

[2] قسم الفيزياء – كلية العلوم- جامعة المنصورة – المنصورة 35516 – مصر

بريد الكترونى : Diaalolo2004@yahoo.com

لقد تم توظيف حسابات النمذجه الجزيئية المعتمدة على ميكانيكا الكم باستخدام نظرية الكثافة الوظيفية (DFT) من خلال طريقة B3LYP وارتكازا على مجموعة اساسات حسابية 6-31g(d,p) لحساب ال single point energy لنترات جزىء البولى انيلين ايمرالدين, بالإضافة الى كبريتات نفس الجزىء. ايضا تم عمل نفس الحسابات على نفس المستوى ل core-shell من البولى انيلين المحيط بالفضة. ومن خلال الحسابات المجراه سالفا تم حساب عزم ثنائى القطبية الكلى لكامل الجزىء مع تحديد اتجاهه فى الفراغ وايضا تم حساب ورسم خريطه لتوزيع الجهد الالكتروستاتيكى الكلى حول الجزيئات محل الدراسة. فى نفس الدراسة وبنفس مستوى الحسابات قمنا بحساب طاقة الفجوه مع رسم الـ HOMO & LUMO لكل جزىء. وقد تم دراسة ايضا تاثير تواجد جزيئات الماء حول الجزيئات محل الدراسه وتاثير زيادة عدد تلك الجزيئات على الخواص سالفة الذكر.